Bull Eng Geol Environ (2016) 75:841–851
DOI 10.1007/s10064-015-0779-9

ORIGINAL PAPER

Utilizing water, mineralogy and sedimentary properties to predict LCPC abrasivity coefficient

Arash Hashemnejad[1] · Mohammad Ghafoori[1] · Sadegh Tarigh Azali[1]

Received: 26 December 2014 / Accepted: 23 July 2015 / Published online: 9 August 2015

Abstract Drilling, blasting and mechanical methods using road headers or tunnel boring machines (TBMs) are among the methods used for underground excavation of rock and soil. The interaction between the tools used and the ground leads to fragmentation of rocks and soil grains as well as tool wear. Wear is defined as the loss of tool material as a result of the interaction between rocks (or soil) and the drilling tools. The LCPC abrasivity test is a quick and easy procedure used widely to assess the abrasivity of soil and rock for predicting the rate of wear of cutting and drilling tools. The LCPC test device is designed to measure the abrasivity of particles as small as fine gravel. Various parameters can affect the LCPC abrasivity coefficient (LAC). In this paper, equations relating the index properties and the LAC were applied to 27 different samples. The derivation of models predicting the engineering geological properties of rocks and soils is useful because providing specimens of rocks at depth is difficult and expensive in the preliminary design of underground projects. Regression analysis was applied in developing some models for the LAC based on indirect methods including the equivalent quartz content (EQC), grain shape, grain size, grain angularity and water saturation applied to data from rock and soil samples in Iran. The results showed that EQC is the most important parameter affecting the LAC, with the other parameters having lower levels of importance.

Keywords LCPC abrasivity coefficient · Tunnel boring machine · Abrasivity · Wear · Equivalent quartz content

✉ Arash Hashemnejad
Hashemnejad.arash@gmail.com

Mohammad Ghafoori
Ghafoori@um.ac.ir

Sadegh Tarigh Azali
sadeghazali@gmail.com

[1] Department of Geology, Ferdowsi University of Mashhad (FUM), Mashhad, Iran

Introduction

The term "abrasiveness" describes the potential of a rock or soil grains to cause wear on a tool (Plinninger and Restner 2008). In abrasive grounds, the wear can occur on several parts of the tunnel boring machine (TBM), including the excavation tools such as the front, rear and periphery of the cutter head, as well as the bulkhead, plunging wall structures and the outlet devices such as screw conveyors on earth pressure balance (EPB)-TBMs (Nilsen et al. 2006a, 2007; Alavi Gharahbagh et al. 2011). The operation often stops immediately upon breaking a tool in order to prevent further damage to other parts. The worn parts (e.g., the jammed disc cutters of a TBM) need to be changed. Thus, ground abrasiveness not only controls the rate of tool wear, but also hinders construction. Consequently, abrasiveness increases project costs and reduces the overall efficiency of the drilling process significantly. Drilling and cutting in surface and underground construction projects are affected significantly by soil abrasiveness (Thuro and Käsling 2009). Wear of the TBM cutter head has been reported in many mechanized tunnelling operations worldwide, such as the ECIS project in Los Angeles, the Elbe Tunnel in Hamburg, Germany (Nilsen et al. 2006b) and Isfahan Metro in Iran (Tarigh Azali and Moammeri 2012). This important effect has also been reported in drilling projects in soft grounds (Alavi

Gharahbagh et al. 2010; Tarigh Azali and Moammeri 2012).

It is generally agreed that abrasivity is one of the most important factors controlling tunnelling in hard rock, affecting both the costs and timing of the project (Büchi et al. 1995). Thus, several tests are carried out to determine the abrasivity of rocks (Käsling and Thuro 2010; Bruland 1998), but measurements of the abrasiveness of soil as a basis for prediction of wear have still not been unified or covered by standards. Various testing processes have not delivered reliable and resilient parameters or contributed to the clarification of disputed matters but have rather been the cause of confusion in the past. Wear estimates based on these methods have also mostly been empirical and thus are based on a high degree of subjective estimation and company-specific experience (Düllmann et al. 2014; Hashemnejad et al. 2012; Thuro 1997). Also, there are currently no recognized prediction models available for the estimation of tool wear in shield tunnelling in soil (Köhler et al. 2011).

Although the extent of soil abrasivity is not similar to that of coarse granular gravel and sand, it can influence significantly the performance of shielded TBMs and large diameter drill holes in soft ground. A reliable prediction of soil abrasiveness in soft ground is invaluable for the designer and the client as well as for contractors estimating the cost of tools and planning for minimizing underground risks.

The LCPC abrasivity testing method for rock and soil, introduced by Laboratoire Central des Ponts et Chaussées (Normalisation Française P18-579 1990) is studied and evaluated in this study. Soil mixtures including different grain sizes can be used in the LCPC abrasivity test (Thuro et al. 2007; Tarigh Azali et al. 2013).

The abrasivity of rocks is controlled by a few well-known parameters, whereas the abrasivity of soils is affected by many parameters, such as the in situ soil conditions (e.g., inhomogeneity, density, and porosity), sedimentary petrology (e.g., mineral composition, roundness and shape of the grains), and technical properties such as the uniaxial comprehensive strength and the abrasivity of grains (Thuro 2002; Plinninger 2002; Thuro and Plinninger 2003; Thuro et al. 2007; Drucker 2011).

The LCPC test

General introduction

The LCPC abrasivity testing device is described based on the French standard of P18-579, 1990 (Fig. 1a). The "abrasimeter" consists of a 750°W strong motor (minimum power) holding a metal impeller that rotates inside a cylindrical vessel that contains a granular sample. The

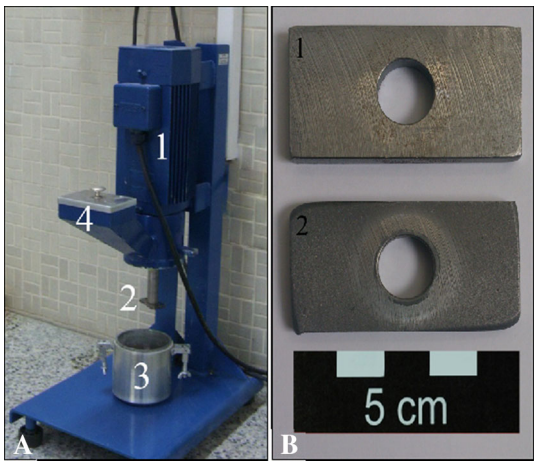

Fig. 1 **a** The LCPC [Laboratoire Central des Ponts et Chaussées (Normalisation Française P18-579 1990)] abrasivity testing device [Ferdowsi University of Mashhad (FUM)]; *1* motor, *2* metal impeller, *3* sample container, *4* funnel tube. **b** Metal impeller (used for orthoclase test, see Fig. 2); *1* before LCPC test, *2* after LCPC test

rectangular impeller is a 50 × 25 × 5 (mm) metal plate that is made of standard steel with a Rockwell hardness of B 60–75 (Fig. 1b). The steel impeller needs to be replaced after each test.

According to the French standard (Normalisation Française P18-579 1990), 500 ± 2 g of an air-dried sample with a 4 mm–6.3 mm fraction is poured into the cylindrical container via a funnel tube. The rectangular metal impeller rotates inside the cylindrical container for 5 min at a speed of 4500 ± 50 rpm. To determine abrasivity, the impeller is weighed before and after the LCPC test. The mass loss of the metal impeller is a measure of the sample's abrasivity, and thus the material property. Clearly, the impeller is subjected to intense abrasion. In addition to mass loss, the metal impeller is deformed as a result of the momentum of the grains rotating within the container. The higher the abrasivity of the sample, the greater the deformation and material loss.

The LCPC abrasivity coefficient (LAC) is expressed as the mass loss of impeller divided by the mass of the sample (500 g).

$$\mathrm{LAC}\,(\text{or } A_{BR}) = \frac{m_0 - m}{M} \tag{1}$$

In the above equation, LAC is the LCPC abrasivity coefficient (g/t), m_0 is the mass of the steel impeller before the LCPC test (g/t), m is the mass of the steel impeller after the LCPC test (g/t) and M is the mass of the sample material (=0.0005 t).

According to Table 1, there are two methods for the classification of soils and rocks based on the LCPC test. The abrasivity of soils and rocks ranges from very low to very high based on LAC values.

Table 1 Classification of the LCPC [Laboratoire Central des Ponts et Chaussées (Normalisation Française P18-579 1990)] abrasivity coefficient (LAC)

Thuro and Käsling (2009)			Büchi et al. (1995)	
LAC (g/t)	Abrasivity classification	Samples	LAC (g/t)	Abrasivity classification
0–50	Not abrasive	Organic materials	<500	Very low
50–100	Not very abrasive	Mudstone, marl	500–1000	Low
100–250	Slightly abrasive	Slate, limestone	1000–1500	Medium
250–500	Abrasive	Schist, sandstone	1500–2000	High
500–1250	Very abrasive	Basalt, quartzitic sandstone	>2000	Very high
1250–2000	Extremely abrasive	Amphibolite, quartzite		

Sample preparation

The LCPC testing device is designed for granular materials in the range of 4–6.3 mm. The coarser grains need to be crushed in advance and their grain fractions need to be determined by sieving. This is due to the diameter of the sample holding container and the dimension of the steel impeller. Although consideration has been given to the construction of larger containers, the technical complexity would be too high (Thuro et al. 2007). The testing of rock material requires that the rock specimen be broken into granular form in a crusher. Subsequently, the sample has to be sieved to obtain the desired grain fraction of between 4 mm and 6.3 mm.

Sample preparation was an important part of this study. An engineering model cannot be interpreted quantitatively by a single sample test. It is also not possible to provide an infinite number of samples for the experiments. Thus, a practical sample collection procedure was planned with the desired impact on the final outcome. Accordingly, the samples were selected based on the criteria specific to each case. In previous studies, the following criteria have been used for the sample selection.

- Providing a framework for understanding the reactions of the samples under different conditions.
- Classifying the different characteristics of samples with similar behaviors.
- The possibility of obtaining quantitative results by studying samples in different conditions.
- The possibility of establishing a relationship between data in order to predict the real conditions encountered in tunnelling with the EPB-TBM.

Establishment of a database

Samples

In this study, 27 samples were prepared. For each type of test, at least two samples were prepared to carry out aggregate abrasion values tests at the Engineering Geology Laboratory of the FUM. The tests were performed according to the AFNOR P18-579 standard. Several samples ready for testing are shown in Fig. 2. These samples were prepared according to the available standards, and their index properties were measured. Measurements of grain size distribution and index sample abrasivity were conducted in accordance with AFNOR P18-553, AFNORP18-579 and AFNOR P18-560 standards, respectively, written for the preparation of test samples, laboratory test procedures and analysis of grain size using laboratory sieves.

Determination of mineralogy and sedimentary parameters

Determination of equivalent quartz content

The equivalent quartz content (EQC) was obtained by multiplying the percentage of the minerals in the rock samples by their Rosiwal abrasiveness values. The EQC of all minerals can be determined by modal analysis (Eq. 2), corresponding to the abrasiveness or hardness of quartz to include all the minerals of a rock sample in each thin section. Therefore, the percentage of each mineral is multiplied by its relative Rosiwal abrasiveness to quartz (Rosiwal 1896, 1916).

$$\mathrm{EQC} = \sum_{i=1}^{n} A_i R_i \tag{2}$$

In the above equation, A is the mineral content (%), R is the Rosiwal abrasiveness (%) and n is the number of minerals.

Determination of grain shape

The shape index (Eq. 3), which is the sum of length-to-width (L/W) and length-to-thickness (L/T) ratios is applied to evaluate the effect of grain shape on abrasivity.

$$\text{Shape index} = \frac{L}{W} + \frac{L}{T} = L\left(\frac{T+W}{W \times T}\right) \tag{3}$$

Fig. 2 A number of samples ready for testing (*left* to *right*: orthoclase, limestone and sandstone); sieve diameters are 21 cm

Table 2 Different types of aggregation used in this study

	Sample 1	Sample 2	Sample 3	Sample 4	Sample 5	Sample 6	Sample 7
Grain size distribution							
d_{min}	4.0	4.0	4.6	5.0	5.4	6.0	6.3
d_{max}	4.0	4.6	5.0	5.4	5.8	6.3	6.3
D_{10}	4.0	4.3	4.7	5.1	5.5	6.1	6.3
D_{30}	4.0	4.4	4.8	5.2	5.6	6.2	6.3
D_{60}	4.0	4.5	4.9	5.3	5.7	6.3	6.3
Effective size	4.0	4.4	4.8	5.2	5.6	6.0	6.3

According to Eq. 3, the shape index varies from 2 (for spherical grains) to 5 (for aciform grains).

Determination of grain size

Seven different categories of grain size are used (Eq. 4) for determining the effect of the grain size on abrasivity. In this equation, D_{10}, D_{30} and D_{60} are the diameters of particles less than 10 %, 30 % and 60 %, respectively, and d_{min} and d_{max} are the minimum and maximum diameters of the tested particles.

$$\text{Effective size} = 0.1\left(\frac{d_{min}+D_{10}}{2}\right)+0.2\left(\frac{D_{10}+D_{30}}{2}\right)+0.3\left(\frac{D_{30}+D_{60}}{2}\right)+0.4\left(\frac{D_{60}+d_{max}}{2}\right) \quad (4)$$

These experimental equations (Eqs. 3, 4) are defined to quantify the effects of grain shape and grain size. According to Eq. 4, seven categories of aggregation are used for elaborating the effect of grain size on abrasivity (Table 2).

Determination of grain angularity

Angularity is a parameter that can be studied in coarse grains. As illustrated in Fig. 3, the grains have been classified into two main classes with high and low sphericity to determine the effect of angularity on the abrasivity. Each class also shows six different types of

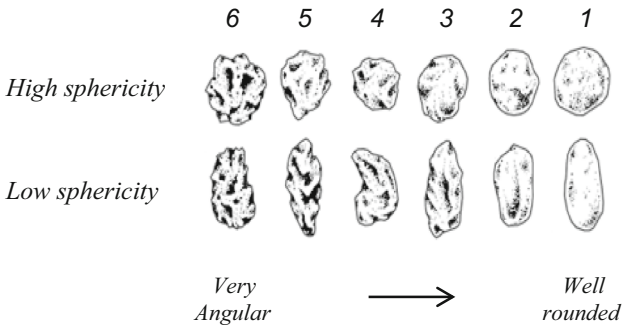

Fig. 3 Differences in grain angularity and sphericity (Tucker 1981); grain types used in this study

Table 3 Average LAC values for the different types of samples used in this study

	Saturation									Shape index				Angularity						Effective size						
	0	10	20	30	40	50	65	80	100	2	3	4	5	1	2	3	4	5	6	4.0	4.4	4.8	5.2	5.6	6.0	6.3
LAC (g/t)																										
Amphibolite	760	840	1020	1120	980	940	880	820	–	760	700	660	600	–	660	700	720	–	760	640	680	700	740	–	800	820
Andalusite	1720	1880	2200	2300	2200	2080	2000	1880	1500	1740	1720	1680	1600	1500	1540	1600	1680	1720	1780	1540	1560	1620	1680	1700	1800	1860
Andesite	1020	1120	1300	–	1300	1260	1180	–	880	1020	980	940	860	880	–	960	980	–	1020	–	940	960	980	1020	1060	1180
Barite	80	80	100	120	100	100	80	80	40	80	80	60	–	–	–	–	80	80	100	40	40	40	60	60	60	60
Basalt	900	1000	1180	–	1160	1120	1040	980	–	900	–	780	720	–	780	800	840	880	900	780	820	840	880	900	940	980
Biotite	40	60	60	60	40	40	40	40	20	–	–	–	40	–	–	–	–	–	–	20	20	20	20	20	20	20
Calcite	300	320	380	400	380	360	360	340	260	280	260	220	180	220	240	280	320	320	340	240	260	260	300	300	340	380
Chromite	800	880	–	1220	1020	1000	920	–	700	800	–	720	640	–	720	740	760	780	800	680	720	–	780	800	–	880
Diorite	1060	–	1380	1440	1460	–	–	–	1000	1060	1020	980	–	–	–	1000	1040	1060	1100	900	960	1000	1020	1060	1120	–
Dolomite	400	440	520	540	500	480	480	440	340	380	360	340	–	–	360	380	400	400	420	340	360	360	380	400	420	420
Fluorite	440	480	580	600	560	520	520	480	360	440	420	360	280	300	300	340	340	400	420	380	400	400	420	440	460	480
Gabbro	1100	–	1340	1500	1420	–	–	–	1000	1080	1020	–	–	–	–	1000	1040	1060	1100	940	960	1000	1040	1100	1180	–
Garnet	1620	1780	2100	2180	2100	1980	1900	1780	1380	1680	1640	1580	–	1380	1420	1500	1560	1600	1660	1440	1480	1520	1580	1620	1700	1760
Gneiss	1520	1680	–	2260	1940	1900	–	–	1320	–	1480	1380	1320	1340	1380	1460	–	1480	1520	1360	1420	1440	–	1520	1620	1680
Granit	980	1080	1280	1440	–	1220	1140	1060	860	980	920	840	820	820	560	880	–	960	980	860	900	–	960	980	1020	–
Gypsum	60	60	80	80	80	–	–	–	40	100	100	80	40	–	–	–	80	80	100	20	20	20	40	40	40	40
Iron	560	620	720	760	680	–	–	–	–	580	540	520	460	460	460	480	500	520	540	500	500	520	540	540	580	600
Limestone	340	380	420	500	440	–	380	380	–	340	320	280	–	240	260	300	320	320	340	–	300	320	320	340	340	360
Marble	420	460	520	560	540	500	480	440	340	380	360	320	240	300	320	360	380	400	420	360	380	380	400	420	440	440
Obsidian	1000	1100	1300	1360	1300	1220	1180	1100	860	980	940	880	780	840	860	900	940	960	1000	880	900	940	980	1000	1040	1080
Opal	1100	1200	1440	1480	1420	1340	1300	1200	940	1000	960	900	800	820	840	880	920	940	980	960	1000	1020	1060	1100	1140	1180
Orthoclase	1320	1460	1720	1780	1720	1600	1560	1460	1120	1400	1360	1300	1260	–	–	1280	1340	1380	1400	1180	1200	1240	1300	1320	1380	1440
Quartz	1740	1920	2260	2360	2240	2120	2060	1900	1560	1760	1700	1660	1580	1560	1600	1640	1680	1700	1740	1580	1620	1680	1740	1760	1860	1920
Quartzite	1580	1740	2060	2360	–	1980	1840	–	1360	1580	1540	1460	–	–	1460	1480	–	1540	1580	–	1460	1500	1540	1580	1680	–
Sandstone	600	660	760	880	760	740	–	660	–	600	540	500	460	480	500	520	540	580	600	520	540	560	560	600	620	640
Stilbite	460	500	580	620	580	500	500	460	380	460	440	400	300	320	340	340	360	400	420	380	380	400	420	460	480	500
Tuff	880	960	1100	1300	–	1100	1020	–	760	880	840	720	–	–	760	820	–	840	880	740	800	840	880	–	940	960

angularity. The grain angularity is expressed by different numbers: from 1 for very rounded to 6 for very angular grains (Fig. 3).

Development of LAC equation

In this study, in order to perform the statistical analyses needed to predict the LAC, we established a database including the EQC, water saturation, effective size, shape index, angularity and the actual values of LAC measured in the laboratory (Table 3).

After establishing the database, a commercial software program for standard statistical analysis was used to perform stepwise and multivariable regression analysis of the known parameters to investigate the unknowns.

Effects of mineralogy and sedimentary parameters on LAC

In order to correlate lithological parameters (EQC, shape index, effective size and angularity) with actually measured LAC values, stepwise statistical analyses were carried out and the influence of each parameter on the LAC was studied.

Literature reports state that the EQC is the most crucial parameter for LAC estimation; however, this study shows that there are more parameters required for predicting the LAC. Likewise, the study shows that the relationship between EQC and LAC is not reliable enough to be used as the only method for predicting soil abrasion. The correlation between EQC and LAC values is presented in Fig. 4.

Shape index According to Fig. 5b, larger grains show higher abrasivity. This can be due to the higher strength of these grains and their stronger impact against the impeller, which causes larger forces to be imparted to the impeller.

Effective size With increasing grain size (Eq. 4) the grains become enlarged in one to three dimensions and, consequently, their strength increases. Thus, the movement of these bigger and stronger grains applies larger forces on the impeller and increases its wear and abrasion (Fig. 5c).

Angularity effect The effect of grain angularity (Fig. 5d) can be determined only in grains with large volumes. Generally, two areas in the impeller are subjected to abrasion in the LCPC tests: the corners and the impeller surface. Grain angularity affects mainly the impeller surface. Angular grains cause more abrasion to the impeller surface and increase the LAC value.

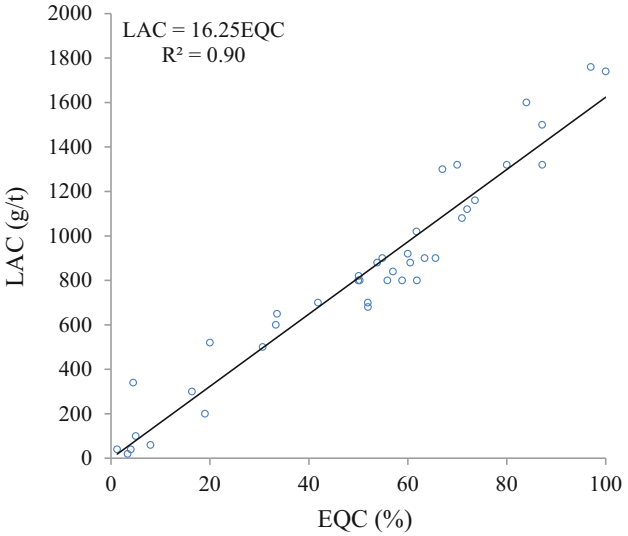

Fig. 4 Correlation between equivalent quartz content (EQC) and LCPC abrasivity coefficient (LAC) values

Effects of water on LAC

The effect of water on the LAC was investigated by adding different amounts of water to the soil. The main impacts of water on the abrasiveness of soil materials can be summarized as follows:

1. First step (up to 35 % water saturation):
   - The water prevents rapid crushing of the grains by reducing the frictional contact between the grains and the impeller.
   - Water prevents the abrasion and crushing of the grains in contact with each other before they collide with the impeller.
   - The water creates adhesion between uncrushed grains and the dust of eroded grains (lumps condensation phenomena).
   - Regular cleaning of the cutting tool is needed to prevent the accumulation of dust on its surface.
2. More than 35 % water saturation:
   - Creates a soil softness effect.
   - Creates an impeller cooling effect.
3. More than 60 % water saturation:
   - This condition leads to an increase in water temperature.
4. Between 75 % and 100 % water saturation:
   - Foam is produced as a result of the water/air mixture.

The soil softness effect depends on the flowing properties and the stickiness of the soil at 35 % to 60 % water saturation. At less than 35 % saturation and higher than 60 % saturation, respectively, flowing and stickiness will disappear. The first and third steps increase and the second and fourth steps decrease the amount of abrasivity. The outcome of each step affects the next step.

According to Fig. 5a, the highest abrasivity of samples occurs at 25–40 % water saturation. For example, the abrasivity of grains with EQC of 75–100 increases by 1.37 % at 35 % water saturation in comparison to dry conditions. Assuming an abrasivity of 1740 g/t for a sample with the EQC of 75–100, the final abrasivity value can be determined from Eq. 5.

$$\frac{\mathrm{LAC}_{W=35}}{\mathrm{LAC}_{W=0}} = 1.37 \xrightarrow{\mathrm{EQC}=75-100\%} \frac{\mathrm{LAC}_{W=35}}{1740} = 1.37 = 1.37 \times 1740 \approx 2380\left(\frac{g}{t}\right) \quad (5)$$

As a result, the water saturation indicates a polynomial form of the relationship with LAC.

Regression analysis

In this statistical approach, five dependent variables (EQC, water, shape, angularity and size) were used as the input parameters and the measured LAC was considered as an independent variable. The impact of each variable on the LAC was evaluated by means of forward stepwise regression analysis.

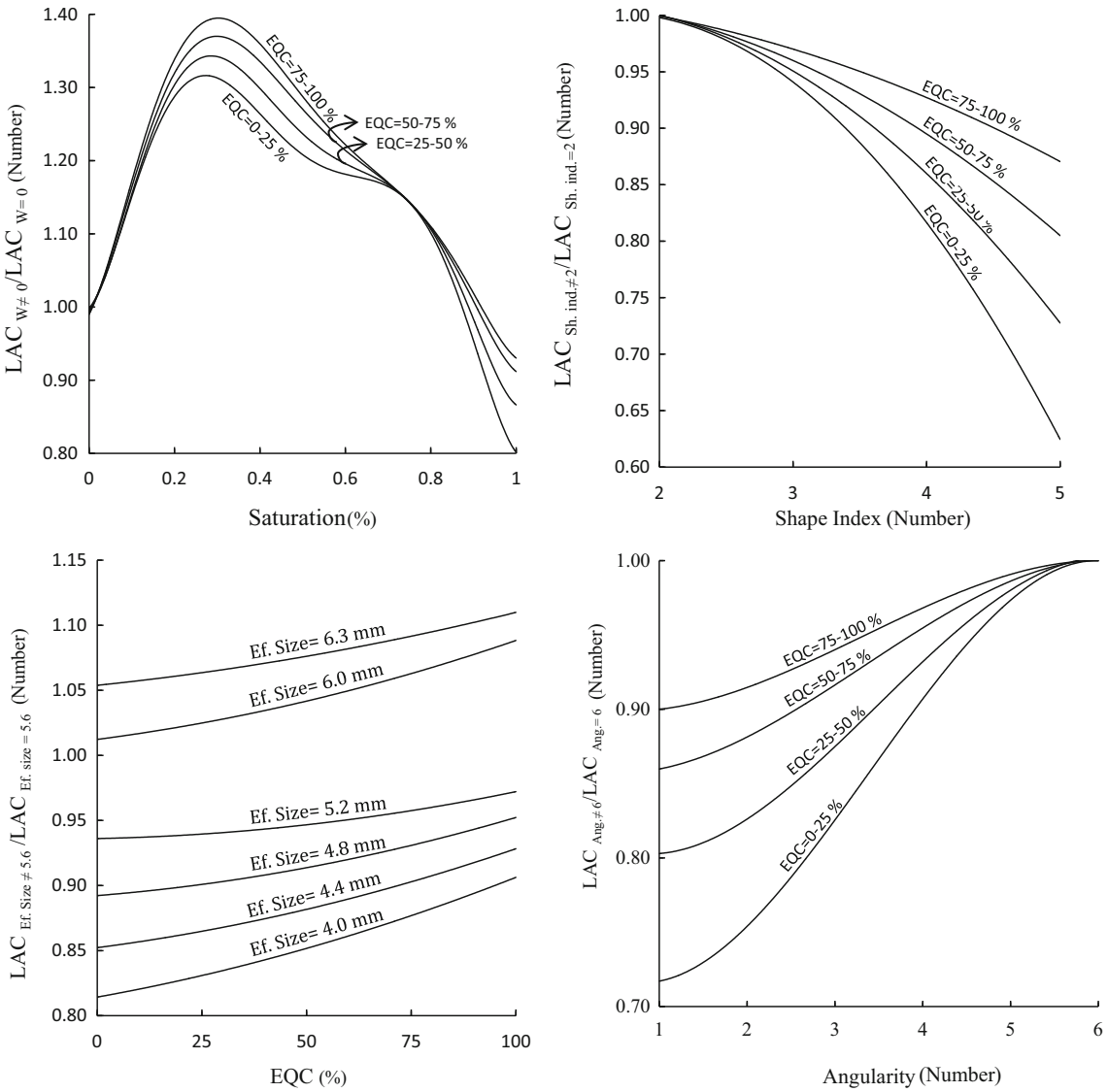

Fig. 5 Relationship between measured LAC and geological parameters

Table 4 α values in different saturation ratios

EQC	α	Equation number
75–100	$36.73\omega^6 - 117.93\omega^5 + 140.78\omega^4 - 73.95\omega^3 + 13.19\omega^2 + 1.11\omega$	6
50–75	$38.66\omega^6 - 122.16\omega^5 + 143.24\omega^4 - 74\omega^3 + 13.11\omega^2 + 1.00\omega$	7
25–50	$50.32\omega^6 - 155.47\omega^5 + 177.40\omega^4 - 89.18\omega^3 + 16.09\omega^2 + 0.69\omega$	8
0–25	$55.35\omega^6 - 168.46\omega^5 + 188.00\omega^4 - 91.71\omega^3 + 15.95\omega^2 + 0.67\omega$	9

Table 5 Variables and summary of the generated models for forward stepwise regression analysis

Model	Variables entered	Method		
1	EQC	Stepwise (criteria: probability-of-*F*-to-enter <0.050, probability-of-*F*-to-remove >0.100)		
2	Size	Stepwise (criteria: probability-of-*F*-to-enter <0.050, probability-of-*F*-to-remove >0.100)		
3	Angularity	Stepwise (criteria: probability-of-*F*-to-enter <0.050, probability-of-*F*-to-remove >0.100)		
4	Shape	Stepwise (criteria: probability-of-*F*-to-enter <0.050, probability-of-*F*-to-remove >0.100)		
Model	*R*	R^2	Adjusted R^2	Std. error of the estimate
Model summary				
1	0.967[a]	0.935	0.934	157.34071
2	0.969[b]	0.940	0.939	151.32324
3	0.975[c]	0.950	0.949	138.15556
4	0.978[d]	0.957	0.957	127.49801

Dependent variable: LAC

EQC Equivalent quartz content

[a] Predictors: (constant), EQC

[b] Predictors: (constant), EQC, size

[c] Predictors: (constant), EQC, size, angularity

[d] Predictors: (constant), EQC, size, angularity, shape

To apply this method, a linear correlation can be assumed between parameters such as EQC, angularity, shape and size. Additionally, the effect of water on abrasivity can be calculated using Eqs. 6–9 in Table 4. Table 4 also illustrates the variation of ω between 0 (dry) and 1 (saturated).

The computer program was used to generate different models with input variables as shown in Table 5. The maximum correlation coefficient ($r = 0.957$) was obtained in Model 4, which is based on the EQC, water saturation, shape, angularity and the size as the input variables. This means that each parameter has a partial effect on the LAC (Table 6). Consequently, the correlations obtained between the variables are actually linear functions. In other words, with a 95 % level of confidence, the program finds the best fitting regression through the parameters in a linear combination. As a result, as a function of measured parameters in Model 4, the LAC predictive equation is obtained empirically as follows (Table 7):

$$\mathrm{LAC}\left(\frac{\mathrm{g}}{\mathrm{t}}\right) = (1+\alpha)(19\mathrm{EQC} - 84\mathrm{Sh} + 123S + 62A - 940) \quad (10)$$

In the above equation, α is the water effect coefficient (Eqs. 6–9 in Table 4) and the EQC is the equivalent quartz content. "Sh", "S" and "A" are indicative of the shape effect, effective size and angularity, respectively.

According to the introduced equation, reliable relationships between the predicted and measured LAC water saturation values were obtained using $r = 0.92$. A comparison between measured and predicted LAC values is shown in Fig. 6.

According to Fig. 5a, in the first section, there is a linear relationship between water saturation and abrasivity (in the range of 0–35 % water saturation). So, to simplify the

Table 6 Stepwise models output and excluded variables from each generated model

	Model	Beta in	*t*	Significance	Partial correlation	Collinearity statistics tolerance
1	Size	0.071[a]	5.769	0.000	0.278	1.000
	Angularity	0.094[a]	7.869	0.000	0.367	0.991
	Shape ef.	−0.068[a]	−5.531	0.000	−0.267	1.000
2	Angularity	0.102[b]	8.960	0.000	0.411	0.983
	Shape	−0.074[b]	−6.287	0.000	−0.301	0.994
3	Shape	−0.088[c]	−8.365	0.000	−0.388	0.979

Dependent variable: LAC

[a] Predictors in the model: (constant), EQC

[b] Predictors in the model: (constant), EQC, size

[c] Predictors in the model: (constant), EQC, size, angularity

Table 7 Significance of coefficients for each generated model

Model	Unstandardized coefficients		Standardized coefficients	*t*	Significance
	B	Std. error	*β*		
1					
(Constant)	−92.161	14.247		−6.469	0.000
EQC	19.102	0.253	0.967	75.437	0.000
2					
(Constant)	−638.566	95.698		−6.673	0.000
EQC	19.105	0.244	0.967	78.450	0.000
Size	99.476	17.243	0.071	5.769	0.000
3					
(Constant)	−1031.916	97.780		−10.554	0.000
EQC	19.297	0.223	0.977	86.390	0.000
Size	112.405	15.808	0.080	7.110	0.000
Angularity	56.036	6.254	0.102	8.960	0.000
4					
(Constant)	−940.225	90.900		−10.344	0.000
EQC	19.341	0.206	0.979	93.797	0.000
Size	123.074	14.645	0.088	8.404	0.000
Angularity	61.942	5.815	0.112	10.653	0.000
Shape	−84.463	10.097	−0.088	−8.365	0.000

Dependent variable: LAC

above equation, the following equation can be employed to obtain abrasivity changes.

$$\mathrm{LAC}\left(\frac{\mathrm{g}}{\mathrm{t}}\right) = 19\mathrm{EQC} + 7\omega - 48\mathrm{Sh} + 66S + 37A - 580 \quad 0 \le \omega \le 35 \tag{11}$$

It should be noted that Eq. 11 is applicable only in ground conditions with up to 35 % water saturation. According to Fig. 5a, water saturation beyond this point affects soil abrasivity and deteriorates the linear correlation between the two parameters. In these circumstances (more than 35 % water saturation), Eq. 12 could be used to determine the amount of abrasivity.

$$\mathrm{LAC}\left(\frac{\mathrm{g}}{\mathrm{t}}\right) = 18\mathrm{EQC} + 0.75\omega - 53\mathrm{Sh} + 72S + 40A - 595 \quad 35 < \omega \le 100 \tag{12}$$

Validation of the generated models

The importance of the coefficients in the correlation (*r* values) can be determined by the *t* test. The test compares the estimated *t* value with a tabulated *t* value using the null hypothesis. According to this hypothesis, if the calculated *t* value is greater than the tabulated *t* value, the null hypothesis that represents the significance of *r* values

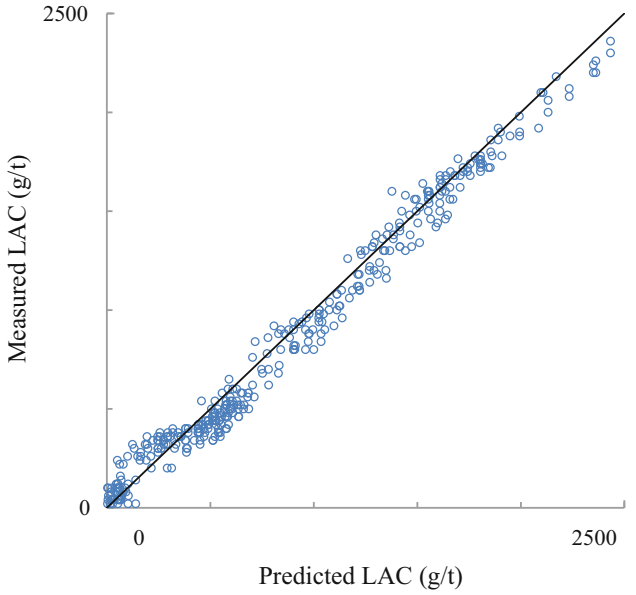

Fig. 6 Comparison between measured LAC and predict LAC (for Eq. 10)

Table 8 Analysis of variance for the significance of regression for each generated model

Model	Sum of squares	*df*	Mean square	*F*	Significance
1					
Regression	1.409E8	1	1.409E8	5690.708	0.000[a]
Residual	9,852,926.826	398	24,756.098		
Total	1.507E8	399			
2					
Regression	1.416E8	2	7.082E7	3092.790	0.000[b]
Residual	9,090,792.604	397	22,898.722		
Total	1.507E8	399			
3					
Regression	1.432E8	3	4.772E7	2500.385	0.000[c]
Residual	7,558,435.575	396	19,086.959		
Total	1.507E8	399			
4					
Regression	1.443E8	4	3.608E7	2219.395	0.000[d]
Residual	6,421,018.728	395	16,255.744		
Total	1.507E8	399			

Dependent variable: LAC

[a] Predictors: (constant), EQC

[b] Predictors: (constant), EQC, size

[c] Predictors: (constant), EQC, size, angularity

[d] Predictors: (constant), EQC, size, angularity, shape

will be rejected; otherwise, it is not significant. All the models have different tabulated *t* values, since each one has a different number of independent variables. As the tabulated *t* values from the reference table indicates, each model works according to the null hypothesis. Model 4 has the highest correlation coefficient and a corresponding critical *t* value of ±2.0423.

In order to test the significance of the performed regressions, an analysis of variance (*F* test) was conducted. All the models have different numbers of independent variables and, as a result, different tabulated *F* values. According to this rule, when the calculated *F* value is greater than the tabulated *F* value, the null hypothesis is rejected. This indicates a real relationship between dependent (actual LAC) and independent (EQC, water saturation, angularity, shape and size) variables and proves that the hypothesis is valid for the models generated. Model 4 has a corresponding critical *F* value of ±2.45 due to the highest correlation coefficient ($r = 0.957$). The variance analysis of models is demonstrated in Table 8.

Conclusions

Data obtained from 27 samples with different EQCs were used to generate an LAC predictive equation as a function of geological parameters including angularity, water, shape effect and effective size. According to the results, EQC, which is highly correlated with the equivalent quartz content, was the most important parameter determining the abrasivity of samples. Additionally, it was demonstrated that water saturation can cause a 30–40 % increase as well as a 10–20 % reduction in the abrasivity of soil grains. Moreover, abrasivity was increased by increasing grain angularity and size and reducing the shape index. It should be noted that these three parameters have a greater impact on abrasivity in samples with higher EQC values.

References

Alavi Gharahbagh EA, Rostami J, Gilbert M (2010) Tool wear issue in soft ground tunnelling, developing a reliable soil abrasivity index. In: Proceedings of the North American Tunnelling Conference, 19–23 June 2010, Portland, OR

Alavi Gharahbagh E, Rostami J, Palomino AM (2011) New soil abrasion testing method for soft ground tunnelling applications. Tunn Undergr Space Technol 26:604–613

Bruland A (1998) PhD thesis. Norwegian University of Science and Technology (NTNU) Trondheim, Norway

Büchi E, Mathier J, Wyss Ch (1995) A significant cost factor for mechanical tunnelling in loose and hard rock. Tunnel 5:38–44

Drucker P (2011) Validity of the LCPC abrasivity coefficient through the example of a recent Danube gravel. Geomech Tunn 4(6):681–691

Düllmann J, Alber M, Plinninger R (2014) Determining soil abrasiveness by use of index tests versus using intrinsic soil parameters. Geomech Tunn 7(1):87–97

Hashemnejad A, Ghafoori M, Lashkaripour G, Tariq Azali S (2012) Effect of geological parameters on soil abrasivity using LCPC machine for predicting LAC. Int J Emerg Technol Adv Eng 2(12):71–76 (ISSN 2250-2459, ISO 9001:2008 Certified Journal)

Käsling H, Thuro K (2010) Determining abrasivity of rock and soil in the laboratory. In: Williams AL, Pinches GM, Chin CY, McMorran TJ, Massey CI (eds) Geologically active. 4600 S., 11th IAEG congress, Auckland, New Zealand, 5–10 September 2010, Paper No. 235, 1973–1980

Köhler M, Maidl U, Martak L (2011) Abrasiveness and tool wear in shield tunnelling in soil (Abrasivität und Werkzeugverschleib beim Schildvortrieb im Lockergestein). Geomech Tunnel 4(1):36–53, Ernst, Berlin

Nilsen B, Dahl F, Holzhäuser J, Raleigh P (2006a) Abrasivity of soils in TBM tunnelling. Tunnels Tunn Int 38(3):36–38

Nilsen B, Dahl F, Holzhäuser J, Raleigh P (2006b) SAT: NTNU's new soil abrasion test. Tunnels Tunn Int 38(5):43–45

Nilsen B, Dahl F, Holzhäuser J, Raleigh P (2007) New test methodology for estimating the abrasiveness of soils for TBM tunnelling. In: Rapid excavation and tunnelling conference (RETC). Toronto, Canada, pp 104–116

Normalisation Française P18-579 (1990) AFNOR Association Française de Normalisation, Paris

Plinninger RJ (2002) Classification and prognosis of tool wear in conventional excavation in hard rock. Munich geological issues, B18, Technical University of Munich

Plinninger RJ, Restner U (2008) Abrasiveness testing, Quo Vadis? A commented overview of abrasiveness testing methods. Geomech Tunn 1(1):61–70

Rosiwal A (1896) Neue Untersuchungs Ergebnisse über die Härte von Mineralien und Gesteinen. Verhandlg K K Geol R-A Wien, 17:475–491

Rosiwal A (1916) Neuere Ergebnisse der Härte Bestimmung von Mineralien und Gesteinen. Ein absolutes Maß für die Härte Spröder Körper. verhandlg d kk geol R-A Wien, pp 117–147

Tarigh Azali S, Ghafoori M, Lashkaripour G, Hassanpour J (2013) Engineering geological investigations of mechanized tunnelling in soft ground: a case study, East–West lot of line 7, Tehran Metro, Iran. Eng Geol 166:170–185

Tarigh Azali S, Moammeri H (2012) EPB-TBM tunnelling in abrasive ground, Esfahan Metro Line 1. WTC ITA-AITES 2012 World Tunnel Congress, Thailand

Thuro K (1997) Drillability prediction Geological influences in hard rock and blast tunnelling. Geol Rundsch 86:426–437

Thuro K (2002) Geological and Rock mechanical fundamental of excavate ability in tunnelling. Munich Geological Issues, B18, Technical University of Munich

Thuro K, Plinninger RJ (2003) Classification and prognosis of performance and wear parameters in tunnelling. Taschenbuch für den Tunnelbau 2003. Gluckauf, Essen

Thuro K, Singer J, Käsling H, Bauer M (2007) Determining abrasiveness with the LCPC Test. In: Proceedings of the 1st Canada—U.S. rock mechanics symposium, Vancouver

Thuro K, Käsling H (2009) Classification of the abrasiveness of soil and rock. Geomech Tunn 2(2):179–188

Tucker ME (1981) Sedimentary petrology. An introduction. Blackwell, Oxford